A Mathematical Model of Bone Remodeling Process: Effect of Vitamin D

Sahattaya Rattanamongkonkul, Wannapa Kunpasuruang, Sittipong Ruktamatakul

and Chontita Rattanakul

***Abstract*—**We propose a system of differential equations in order to investigate bone remodeling process based on the effect of vitamin D. The model is then analyzed by using singular perturbation technique in order to identify different dynamic behaviors exhibited by the model. Numerical simulations are also carried out to support our theoretical predictions. Both of theoretical and numerical results show that the model can exhibit a periodic behavior corresponds to the pulsatile serum level of vitamin D observed in the clinical evidence.

***Keywords*—**bone formation, bone resorption, singular perturbation, mathematical model, vitamin D.

I. Introduction

VITAMIN D is a steroid vitamin, a group of fat-soluble prohormones which can be obtained from exposure to sunlight or vitamin D supplements. The active form of vitamin D is calcitriol. Calcitriol is synthesized in kidneys and circulates as a hormone. It plays an important role in regulating the concentration of calcium and phosphate in the bloodstream and promoting the healthy growth and remodeling of bone [1]. Calcitriol mediates its biological effects by binding to the vitamin D receptor (VDR), which is principally located in the nuclei of target cells [2]. In bone remodeling process, calcitriol interacts with its VDR in osteoblast (bone forming cell) resulting in the expression of RANKL which recognized by its corresponding receptor RANK on the preosteoclast. The interaction of RANKL and RANK results in signal transduction inducing the preosteoclast to be come a mature osteoclast (bone resorbing cell) [3]-[5].

The purposes of bone remodeling process are to regulate calcium homeostasis, to repair micro-damaged bones and also to shape and sculpture the skeleton during growth [6]-[8]. The process begins with the appearance of osteoclasts on the surface of an inactive surface of bone after that osteoclasts resorb bone and liberates calcium into blood. The resorption cavity will then be refilled by osteoblasts. If the imbalance between the resorption and formation of bone occurs after each remodeling cycle the degree of bone loss will be increased and that leads to osteoporosis [7]-[8]. In this paper, we will propose a mathematical model to describe bone remodeling based on the effect of vitamin D.

II. Model Development

Let us denote the serum level of vitamin D at time t by $X(t)$, the number of active osteoclasts at time t by $Y(t)$, and the number of active osteoblasts at time t by $Z(t)$. We also assume that the high levels of osteoclast and osteoblast precursors lead to the high levels of active osteoclastic and osteoblastic cells, respectively, which result from the differentiation, and activation of their precursors.

Firstly, vitamin D plays an important role in calcium homeostasis. The efficiency of intestinal calcium absorption increases as the serum level of vitamin D increases. Vitamin D enlarges the mobilization of stem cells to become osteoclasts resulting in the increase in the release of calcium from bone [9]-[12]. Hence, the equation for the rate of change in serum level of vitamin D is then assumed to have the form

$$\frac{dX}{dt} = \frac{a_1}{k_1 + Y} - b_1 X \tag{1}$$

where the first term on the right-hand side of (1) represents the rate of change in serum level of vitamin D which decreases with the increase in the number of active osteoclasts in order to counter balance the high level of calcium in blood resulted from the large number of active osteoclasts. The last term is the removal rate constant b_1. a_1 and k_1 are positive constants.

Manuscript received July 31, 2011. This work was supported by the Centre of Excellence in Mathematics, Commission on Higher Education, Thailand and the Faculty of Science, Mahidol University, Thailand.

S. Rattanamongkonkul is with the Department of Mathematics, Faculty of Science, Burapha University, Thailand and the Centre of Excellence in Mathematics, the Commission on Higher Education, Thailand (e-mail: sahattay@buu.ac.th).

W. Kunpasuruang is with the Department of Mathematics, Faculty of Science, Silpakorn University, Thailand and the Centre of Excellence in Mathematics, the Commission on Higher Education, Thailand (e-mail: wannapa@su.ac.th).

S. Ruktamatakul is with the Department of Mathematics, Faculty of Liberal Arts Science, Kasetsart University, Thailand and the Centre of Excellence in Mathematics, the Commission on Higher Education, Thailand (e-mail: faasspr@nontri.ku.ac.th).

C. Rattanakul is with the Department of Mathematics, Faculty of Science, Mahidol University, Thailand and the Centre of Excellence in Mathematics, the Commission on Higher Education, Thailand (corresponding author, phone: 662-201-5340; fax: 662-201-5343; e-mail: sccrt@mahidol.ac.th).

Secondly, osteoclasts are derived from the hemopoietic cells. The hemopoietic stem cells proliferate osteoclast progenitors or preosteoclast precursor cells and then preosteoclasts precursors differentiate into preosteoclasts. After that, preosteoclasts differentiate into osteoclasts [13]. The works of Kong *et al.* [14], Takahashi *et al.* [15] and Burgess *et al.* [16] suggested that the differentiation of osteoclasts requires the presence of osteoblasts and their precursors which respond to hormones and paracrine messengers necessary for the differentiation of osteoclasts. The responsiveness of osteoblasts and their precursors to those necessary factors then regulates the responsiveness of preosteoclasts and osteoclasts. Therefore, the dynamics of the active osteoclastic population can be described by the following equation

$$\frac{dY}{dt} = \left(\frac{a_2 + a_3 X}{k_2 + X^2} \right) YZ - b_2 Y \tag{2}$$

where the first term on the right-hand side of (2) represents the stimulating effect of vitamin D on the reproduction of active osteoclasts through the interaction of vitamin D and its receptors on osteoblasts resulting in the expression of RANKL. The interaction of RANKL on osteoblasts and RANK on preosteoclasts leads to the differentiation of preosteoclasts to osteoclasts [3]-[5]. The last term is the removal rate constant b_2. a_2, a_3 and k_2 are positive constants.

Finally, osteoblasts are derived from mesenchymal cells. The stromal stem cells proliferate osteoprogenitors or preosteoblast precursors and then preosteoblasts precursors proliferate preosteoblasts. After that, preosteoblasts differentiate into osteoblats [13]. There are many factors involving in the proliferation and differentiation of osteoblasts such as FGF, IGF-I, TGF-beta including vitamin D [17], [18]. The dynamics of the osteoblastic population can then be described by the following equation

$$\frac{dZ}{dt} = a_4 + \frac{a_5 XZ}{k_3 + X} - b_3 Z \tag{3}$$

where the first term on the right-hand side of (3) represents the stimulating effect of many factors such as FGF, IGF-I, TGF-beta on the proliferation and differentiation of active osteoblasts. The second term on the right-hand side of (3) represents the stimulating effect of vitamin D on the reproduction of active osteoblastic cells. The last term is the removal rate constant b_3. a_4, a_5 and k_3 are positive constants.

III. Model Analysis

We assume that the dynamics of the changes in serum level of vitamin D is the fastest one. The osteoclastic population possesses the intermediate dynamics and the osteoblastic population has the slow dynamics. We then scale the dynamics of the three components and parameters of the system in term of small positive parameters $0 < \varepsilon << 1$ and $0 < \delta << 1$ as follows.

Letting $x = X$, $y = Y$, $z = Z$, $c_1 = a_1$, $c_2 = \frac{a_2}{\varepsilon}$, $c_3 = \frac{a_3}{\varepsilon}$, $c_4 = \frac{a_4}{\varepsilon\delta}, c_5 = \frac{a_5}{\varepsilon\delta}, d_1 = b_1, d_2 = \frac{b_2}{\varepsilon}, d_3 = \frac{b_3}{\varepsilon\delta}$, we are led to the following model equations:

$$\frac{dx}{dt} = \frac{c_1}{k_1 + y} - d_1 x \equiv f(x, y, z) \tag{4}$$

$$\frac{dy}{dt} = \varepsilon \left(\left(\frac{c_2 + c_3 x}{k_2 + x^2} \right) yz - d_2 y \right) \equiv \varepsilon g(x, y, z) \tag{5}$$

$$\frac{dz}{dt} = \varepsilon\delta \left(c_4 + \frac{c_5 xz}{k_3 + x} - d_3 z \right) = \varepsilon\delta h(x, y, z) \tag{6}$$

which means that during transitions, when the right sides of equations (4)-(6) are finite but different from zero, $|\dot{y}|$ is of the order ε and $|\dot{z}|$ is of the order $\varepsilon\delta$. The shapes and relative positions of the manifolds $\{f = 0\}, \{g = 0\}$ and $\{h = 0\}$ determine the shapes, directions and speeds of the solution trajectories. We now analyze each of the equilibrium manifolds in detail.

The manifold $\{f = 0\}$

This manifold is given by the equation

$$x = \frac{1}{d_1} \left(\frac{c_1}{k_1 + y} \right) \equiv A(y) \tag{7}$$

which is independent of the variable *z* and thus parallels to the z-axis. It intersects the $(x,z)-$plane along the line

$$x = \frac{c_1}{d_1 k_1} \equiv x_1 \tag{8}$$

Moreover, $A(y)$ is a decreasing function of *y* and $A(y) \to 0$ as $y \to \infty$.

The manifold $\{g = 0\}$

This manifold consists of two submanifolds. One is the trivial manifold $y = 0$. The nontrivial one given by the equation

$$z = \frac{d_2 \left(k_2 + x^2 \right)}{c_2 + c_3 x} \equiv B(x) \tag{9}$$

this nontrivial manifold is independent of the variable y and thus this submanifold is parallel to the *y*-axis. It attains the relative minimum at the point where

$$x = \frac{-c_2 + \sqrt{c_2^2 + c_3^2 k_2}}{c_3} \equiv x_m \tag{10}$$

and

$$z = \frac{d_2 \left(k_2 + x_m^2 \right)}{c_2 + c_3 x_m} \equiv z_m \tag{11}$$

On the other hand, the nontrivial manifold intersects the (*y*,*z*)-plane along the line

$$z = \frac{d_2 k_2}{c_2} \equiv z_1 \tag{12}$$

Moreover, the manifold $\{f = 0\}$ intersects the trivial manifold $\{g = 0\}$ along the line $x = x_1$ on the (*x*,*z*)-plane and it intersects the nontrivial manifold $\{g = 0\}$ along the curve

$$z = \frac{d_2\left(k_2 + A(y)^2\right)}{c_2 + c_3 A(y)} \tag{13}$$

which has a relative minimum point $N(x_m, y_m, z_m)$ where

$$y_m = \frac{c_1}{d_1 x_m} - k_1 \tag{14}$$

Also, the curve $\{f = g = 0\}$ intersects the (*x*,*z*)-plane at the point *U* where $y = 0, x = x_1$ and

$$z = \frac{d_2\left(k_2 + x_1^2\right)}{c_2 + c_3 x_1} \equiv z_2 \tag{15}$$

The manifold $\{h = 0\}$

This manifold is given by the equation

$$z = \frac{c_4 x + c_4 k_3}{(d_3 - c_5)x + d_3 k_3} \equiv C(x) \tag{16}$$

which is independent of the variable *y*, and thus parallels to the *y*-axis. It intersects the (*y*,*z*)-plane along the line

$$z = \frac{c_4}{d_3} \equiv z_3 \tag{17}$$

and intersects the (x,z)-plane along a curve which is asymptotic to the line

$$x = \frac{d_3 k_3}{c_5 - d_3} \equiv x_2 \tag{18}$$

We note that $x_2 > 0$ if and only if

$$d_3 < c_5 \tag{19}$$

We also observe that $C(x)$ is an increasing function of *x*.

Moreover, the trivial manifold $\{g = 0\}$ intersects the manifold $\{h = 0\}$ along the curve

$$z = \frac{d_2\left(k_2 + x^2\right)}{c_2 + c_3 x}$$

on the (*x*,*y*)-plane and the nontrivial manifold $\{g = 0\}$ intersects the manifold $\{h = 0\}$ along the line

$$\left\{x = x_3, z = \frac{c_4 x_3 + c_4 k_3}{(d_3 - c_5)x_3 + d_3 k_3} \equiv z_4\right\}$$

which is parallel to the *y*-axis, x_3 being the real solution of

$$d_2(d_3 - c_5)x^3 + (d_2 d_3 k_3 - c_3 c_4)x^2 + \left(d_2 k_2 (d_3 - c_5) - c_2 c_4 - c_3 c_4 k_3\right)x + (d_2 d_3 k_2 k_3 - c_2 c_4 k_3) = 0$$

which exists in the positive octant and is unique provided that

$$\frac{c_2 c_4}{k_2} < d_2 d_3 < \frac{c_3 c_4}{k_3} \tag{20}$$

On the other hand, the manifold $\{h = 0\}$ intersects the (*x*,*z*)-plane along the curve $z = C(x)$ which intersects the line $x = x_1$ at the point $S_1(x_1, 0, z_5)$ where

$$z_5 = \frac{c_4 x_1 + c_3 k_3}{(d_3 - c_5)x_1 + d_3 k_3} \tag{21}$$

The curve $\{f = g = 0\}$ intersects the curve $\{g = h = 0\}$ at the point $S_2(x_3, y_1, z_5)$ where

$$y_1 = \frac{c_1}{d_1 x_3} - k_1 \tag{22}$$

We now identify and analyze each of the three possible cases as shown in Fig. 1 through Fig. 3 as follows.

Case I: If ε and δ are sufficiently small and the inequalities (19) and (20) hold and

$$x_m < x_3 < x_1 \tag{23}$$

and

$$z_3 < z_m < z_2 < z_5 < z_1 \tag{24}$$

where all the parametric values are given as above, then the manifolds are positioned as in Fig. 1 and the system of (4)-(6) will have a periodic solution. Here, the transitions of slow, intermediate and high speeds are indicated by one, two and three arrows, respectively.

In Fig. 1, without loss of generality, we start from point *I* and we assume that the position of *I* is as in Fig. 1 with $\{f \neq 0\}$. A fast transition will bring the solution trajectory to point *J* on the manifold $\{f = 0\}$. Here, $\{g < 0\}$ and a transition at intermediate speed will be made in the direction of decreasing y until point *K* on the curve $\{f = g = 0\}$ is reached. A slow transition then follows along this curve to some point *L* where the stability of submanifold will be lost. A jump to point *M* on the other stable part of $\{f = g = 0\}$ followed by a slow transition in the direction of decreasing z until the point *N* is reached since $\{h < 0\}$ here. Once the point *N* is reached the stability of submanifold will be lost. A jump to point *O* on the other stable part of $\{f = g = 0\}$ followed by a slow transition in the direction of increasing *z* since $\{h > 0\}$ here. Consequently, a slow transition will bring the system back to the point *L*, followed by flows along the same path repeatedly, resulting in the closed orbit *LMNOL*. Thus, limit cycle in the system for ε and δ are sufficiently small exists.

The above analysis can be summarized as in the following theorem.

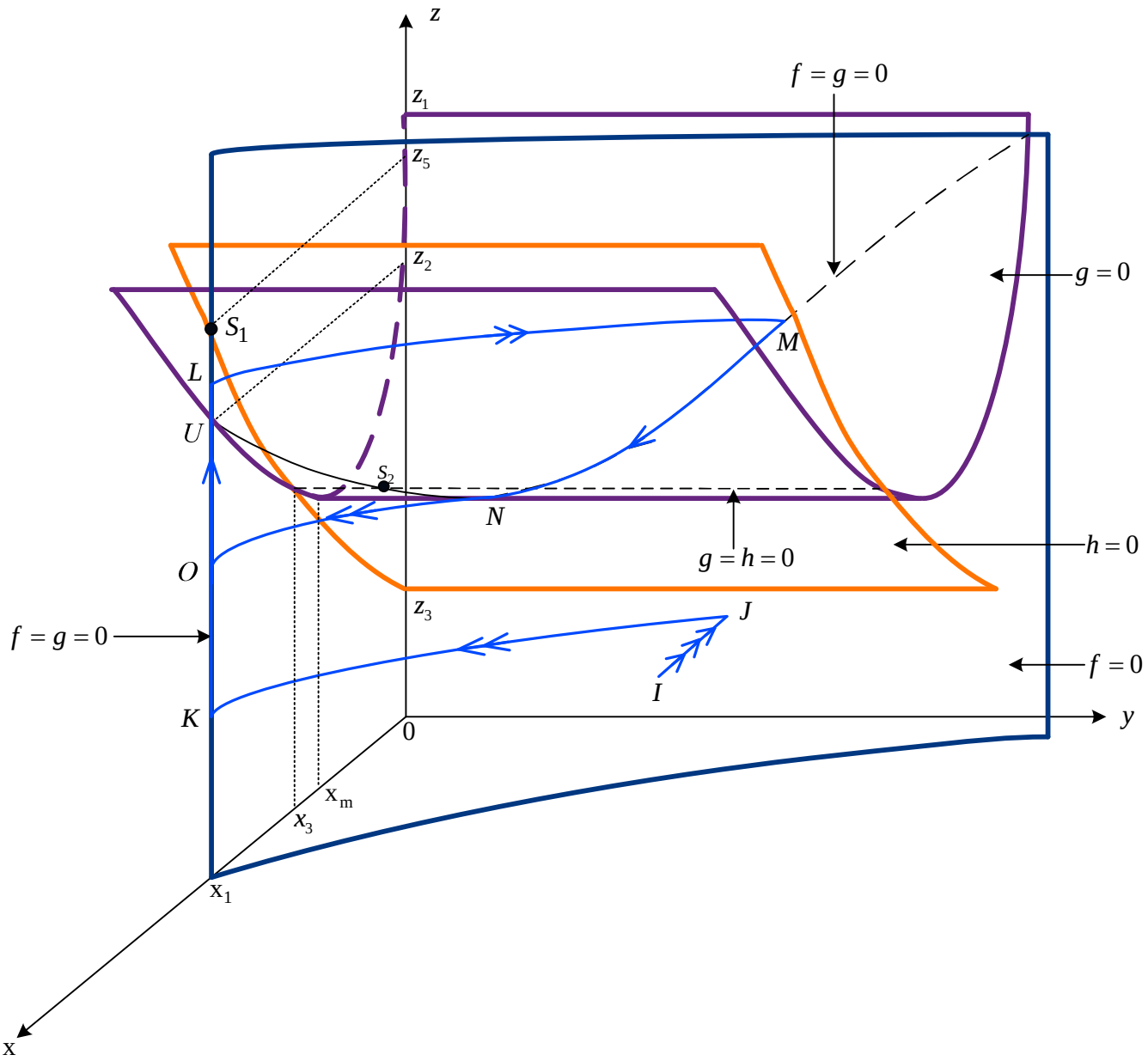

Fig. 1 The three equilibrium manifolds $\{f=0\},\{g=0\}$ and $\{h=0\}$ in the (x,y,z) – space in the Case 1. Segments of the trajectories with one, two, and three arrows represent slow, intermediate, and fast transitions, respectively.

Case II: In this case, the inequality (20) is violated. If ε and δ are sufficiently small and the inequalities (19) holds and

$$x_m < x_1 \tag{25}$$

and

$$z_3 < z_m \tag{26}$$

where all the parametric values are given as above, then the manifolds are positioned as in Fig. 2 and the system of (4)-(6) will have a stable equilibrium point.

In Fig. 2, without loss of generality, we start from point I and we assume that the position of I is as in Fig. 2 with $\{f \neq 0\}$. A fast transition will bring the solution trajectory to point J on the manifold $\{f=0\}$. Here, $\{g<0\}$ and a transition at intermediate speed will be made in the direction of decreasing y until point K on the curve $\{f=g=0\}$ is reached followed by a slow transition in the direction of increasing z until the steady state S_1 where $f=g=h=0$ is reached since $\{h>0\}$ here. Thus, the solution trajectory is expected in this case to tend toward this stable equilibrium point S_1 as time passes.

Case III: If ε and δ are sufficiently small and the inequalities (19) and (20) hold and

$$x_3 < x_m < x_1 \tag{27}$$

and

$$z_m < z_3 < z_1 \tag{28}$$

where all the parametric values are given as above, then the manifolds are positioned as in Fig. 3 and the system of (4)-(6) will have a stable equilibrium point.

In Fig. 3, without loss of generality, we start from point I and we assume that the position of I is as in Fig. 3 with $\{f \neq 0\}$. A fast transition will bring the solution trajectory to point J on the manifold $\{f = 0\}$. Here, $\{g < 0\}$ and a transition at intermediate speed will be made in the direction of decreasing y until point K on the curve $\{f = g = 0\}$ is reached. A slow transition then follows along this curve to some point L where the stability of submanifold will be lost. A jump to point M on the other stable part of $\{f = g = 0\}$ followed by a slow transition in the direction of decreasing z until steady state S_2 where $f = g = h = 0$ is reached since $\{h < 0\}$ here. Thus, the solution trajectory is expected in this case to tend toward this stable equilibrium point S_2 as time passes.

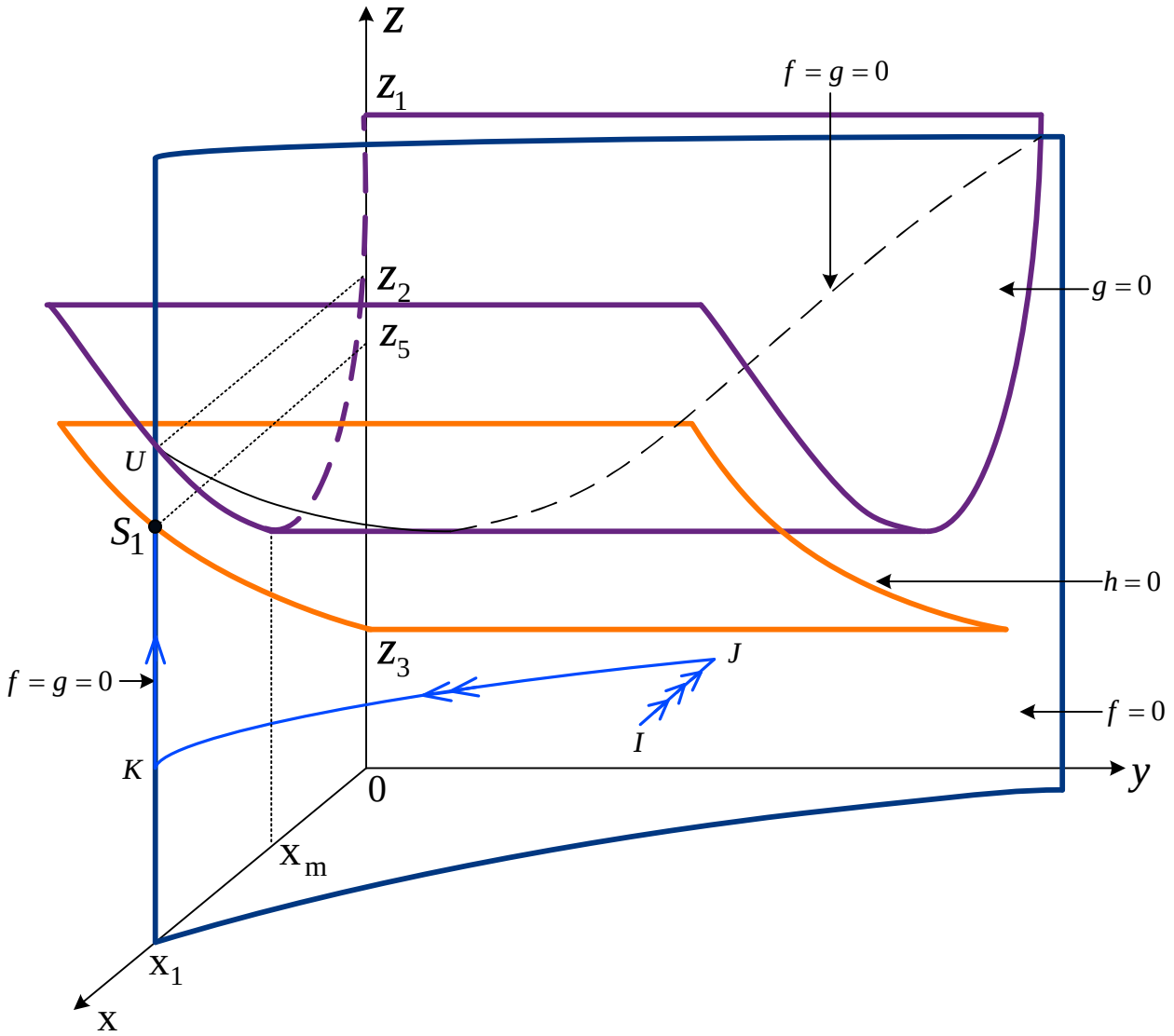

Fig. 2 The three equilibrium manifolds $\{f = 0\}, \{g = 0\}$ and $\{h = 0\}$ in the (x, y, z) – space in the Case 2. Segments of the trajectories with one, two, and three arrows represent slow, intermediate, and fast transitions, respectively.

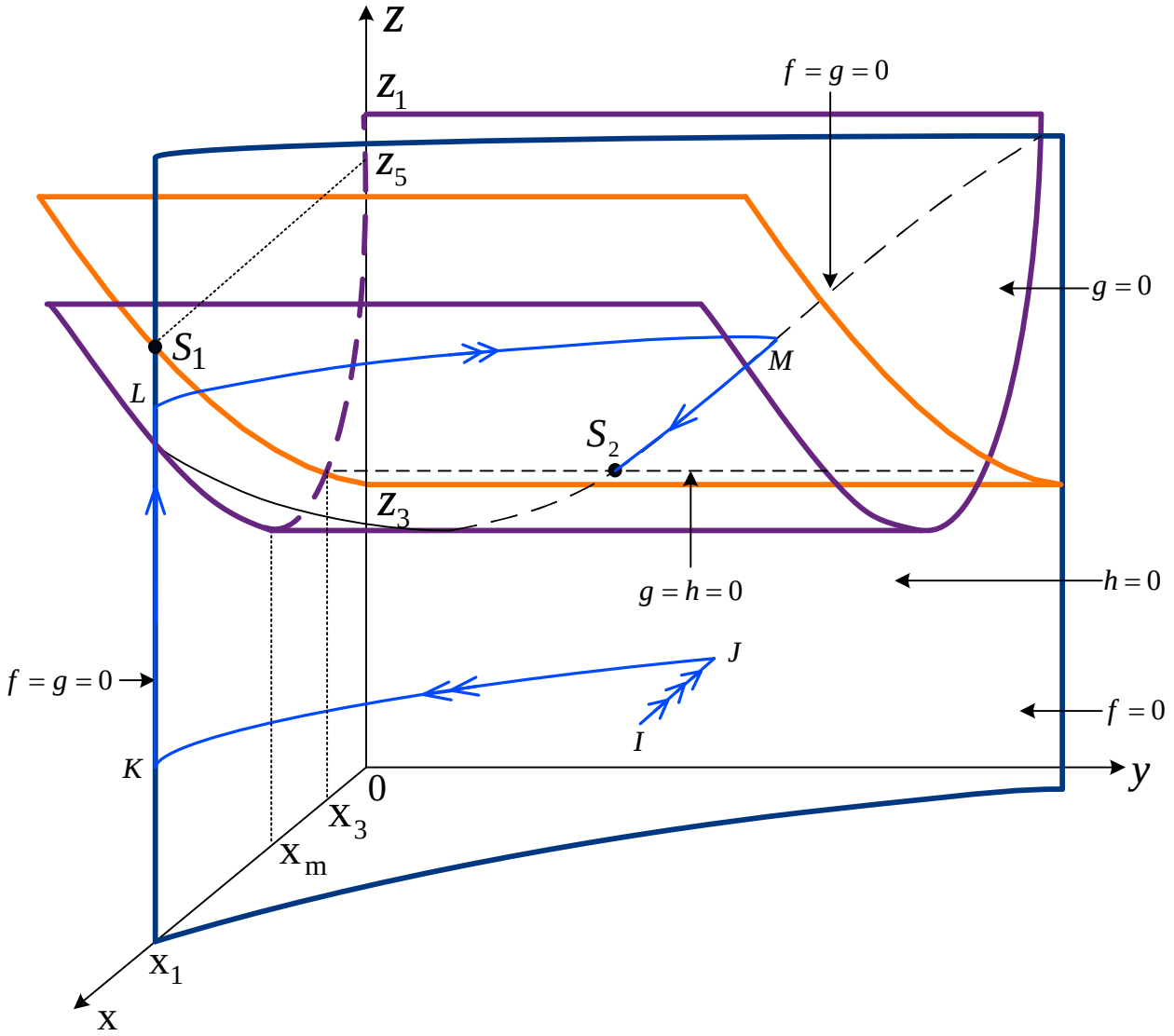

Fig. 3 The three equilibrium manifolds $\{f=0\},\{g=0\}$ and $\{h=0\}$ in the $(x,y,z)-$space in the Case 3. Segments of the trajectories with one, two, and three arrows represent slow, intermediate, and fast transitions, respectively.

IV. NUMERICAL RESULT

A computer simulation of the system (4)-(6) with parametric values chosen to satisfy the condition in Case 1 is presented in Fig. 4. The solution trajectory, shown in Fig. 4a project onto the (x,y)-plane, tends to a periodic solution as theoretically predicted. The corresponding time courses of the level of serum vitamin D, the number of active osteoclasts and the number of active osteoblasts are as shown in Fig. 4b, 4c and 4d, respectively.

A computer simulation of the system (4)-(6) with parametric values chosen to satisfy the condition in Case 2 is presented in Fig. 5. The solution trajectory, shown in Fig. 5a project onto the (x,y)-plane, tends to a stable equilibrium as theoretically predicted. The corresponding time courses of the level of serum vitamin D, the number of active osteoclasts and the number of active osteoblasts are as shown in Fig. 5b, 5c and 5d, respectively.

A computer simulation of the system (4)-(6) with parametric values chosen to satisfy the condition in Case 3 is presented in Fig. 6. The solution trajectory, shown in Fig. 6a project onto the (x,y)-plane, tends to a stable equilibrium as theoretically predicted. The corresponding time courses of the level of serum vitamin D, the number of active osteoclasts and the number of active osteoblasts are as shown in Fig. 6b, 6c and 6d, respectively.

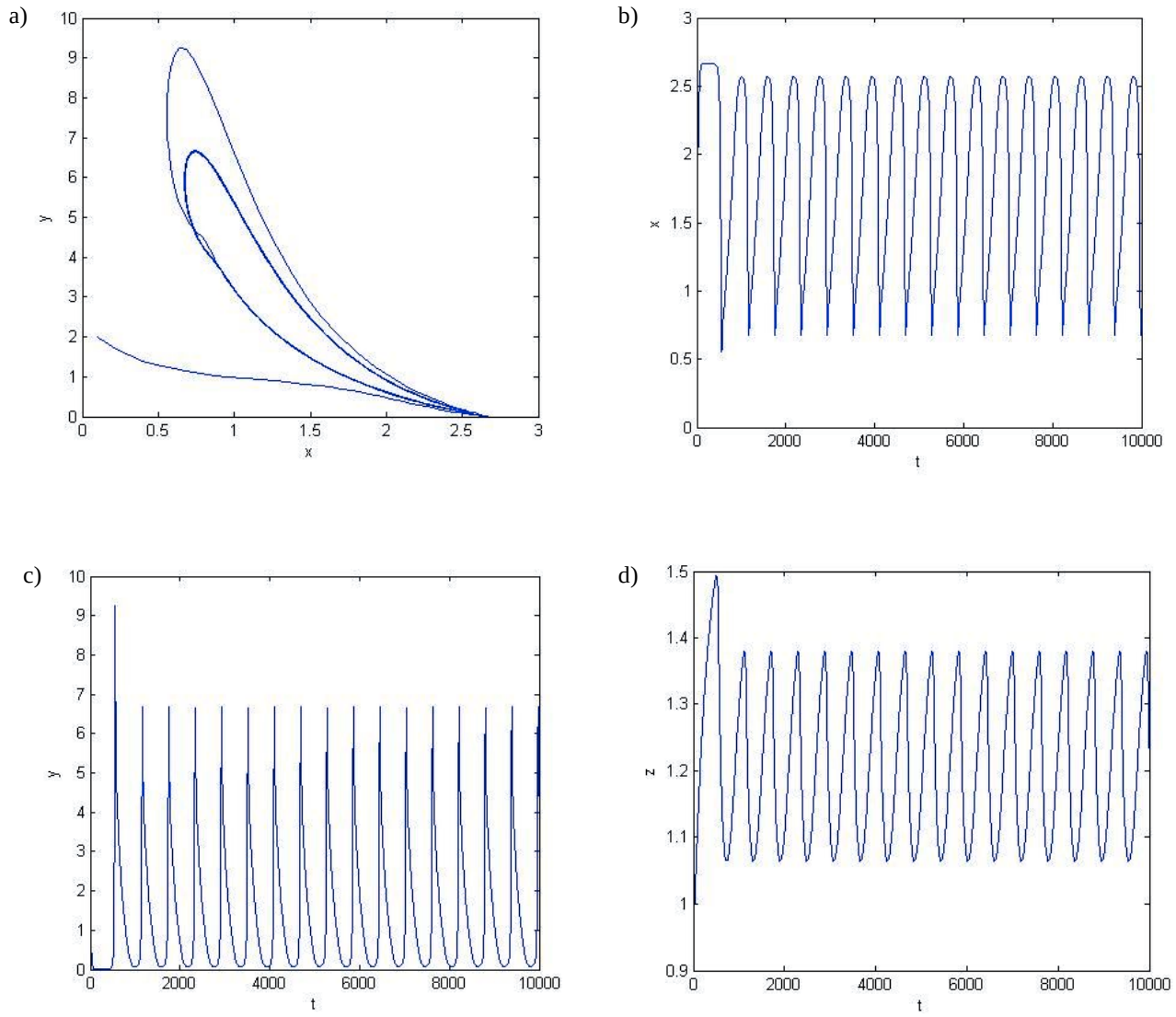

Fig. 4 A computer simulation of the model systems (4)-(6) with $c_1 = 0.8, c_2 = 0.01, c_3 = 0.9, c_4 = 0.3, c_5 = 0.71$, $k_1 = 2$, $k_2 = 2$, $k_3 = 1$, $d_1 = 0.15$, $d_2 = 0.35$, $d_3 = 0.7$, $\varepsilon = 0.9$, $\delta = 0.02$, $x(0) = 0.1, y(0) = 2$, and $z(0) = 1$. (a) The solution trajectory projected onto the (x,y)-plane. (b) The corresponding time courses of the level of serum vitamin D (x), (c) number of active osteoclastic cells (y), and (d) number of active osteoblastic cells (z).

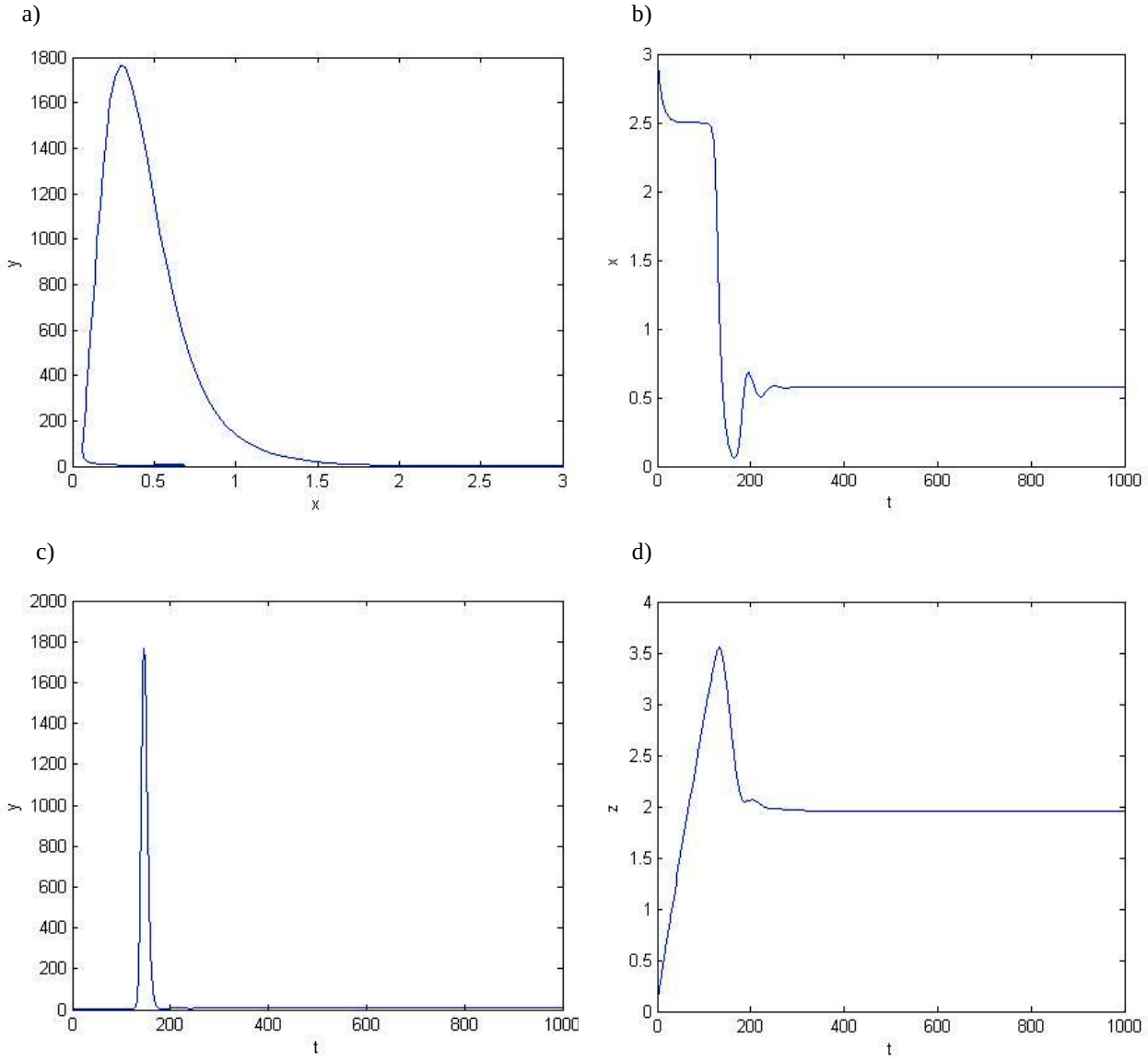

Fig. 5 A computer simulation of the model systems (4)-(6) with $c_1 = 0.5, c_2 = 0.01, c_3 = 0.6, c_4 = 0.3, c_5 = 0.4$, $k_1 = 2$, $k_2 = 2$, $k_3 = 1$, $d_1 = 0.1$, $d_2 = 0.3$, $d_3 = 0.3$, $\varepsilon = 0.5$, $\delta = 0.02$, $x(0) = 5, y(0) = 2,$ and $z(0) = 1$. (a) The solution trajectory projected onto the (x,y)-plane. (b) The corresponding time courses of the level of serum vitamin D (x), (c) number of active osteoclastic cells (y), and (d) number of active osteoblastic cells (z).

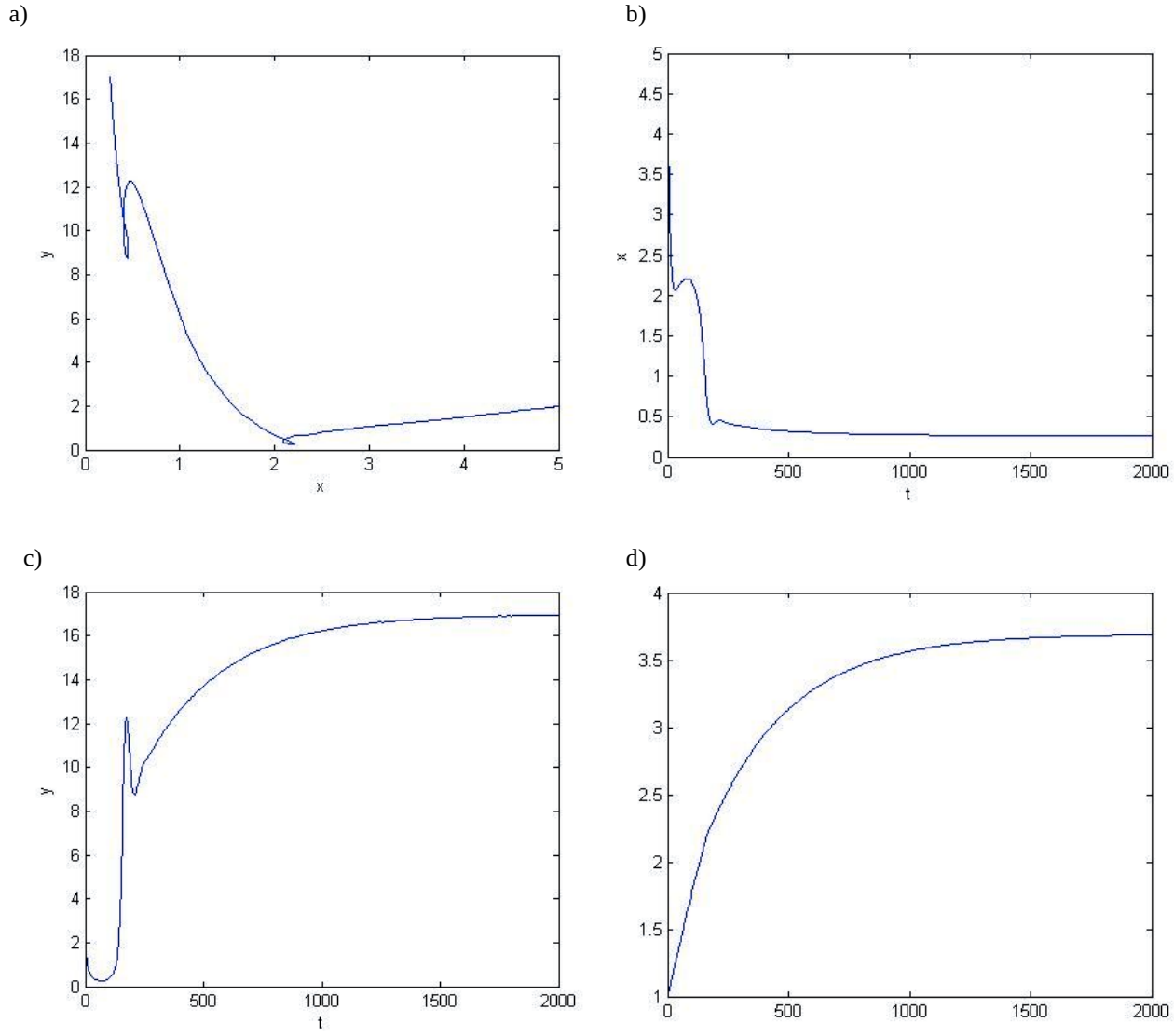

Fig. 6 A computer simulation of the model systems (4)-(6) with $c_1 = 0.5, c_2 = 0.01, c_3 = 0.6, c_4 = 0.8, c_5 = 0.4$, $k_1 = 2$, $k_2 = 2$, $k_3 = 1$, $d_1 = 0.1$, $d_2 = 0.3$, $d_3 = 0.3$, $\varepsilon = 0.5$, $\delta = 0.02$, $x(0) = 5, y(0) = 2,$ and $z(0) = 1$. (a) The solution trajectory projected onto the (x,y)-plane. (b) The corresponding time courses of the level of serum vitamin D (x), (c) number of active osteoclastic cells (y), and (d) number of active osteoblastic cells (z).

V. CONCLUSION

In this paper, bone remodeling process is investigated mathematically. We have proposed and analyzed a system of nonlinear differential equations accounting for the level of vitamin D, the number of active osteoclasts, and the number of active osteoblasts as in (1)-(3). The singular perturbation technique [19], [20] has been used to obtain the conditions on the system parameters for which the various kinds of dynamics behavior can be occurred including a periodic behavior in the solution of the system. Numerical simulations of the model are then carried out by using Runge-Kutta method which has been widely use to find the approximate solution of the differential equations [21]-[24]. The result shows that our model can deduce the nonlinear dynamic behavior which closely resembles to the serum level of vitamin D that has been observed clinically [25], [26], even though the model is kept relatively simple.

REFERENCES

[1] M.D. Van, H.A.P. Pols and J.P.T.M.V. Leeuwen, "Osteoblast differentiation and control by vitamin D and vitamin D metabolites", *Curr. Pharmacl. Design*, vol.10, no.21, pp.2535-2555, 2004.

[2] Standing Committee on the Scientific Evaluation of Dietary Reference Intakes, Food and Nutrition Board, Institute of Medicine, *Dietary reference intakes: for calcium, phosphorus, magnesium, vitamin D and fluoride*, Washington, D.C: National Academy Press. 1997. pp. 250-287.

[3] M.F. Holick, "Vitamin D: importance in the prevention of cancers, type 1 diabetes, heart disease, and osteoporosis", *Am. J. Clin. Nutr*., vol. 79, pp. 362-371, 2004.

[4] S. Khosla, "The OPG/RANKL/RANK system", *Endocrinology*, vol. 142, pp. 5050-5055, 2001.

[5] M.F. Holick, "Vitamin D: Important for prevention of osteoporosis, cardiovascular heart disease, type 1 diabetes, autoimmune disease, and some cancers", *Southern Med. J*., vol. 98, no. 10, pp. 1024-1027, 2005.

[6] T.K. Lewellen, W.B. Neip, R. Murano, G.M. Hinn and C.H. Chesnut, "Absolute Measurement of Total-Body Calcium by the Ar-37 Method- Preliminary Results:Concise Communication", *J. Nucl. Med*., vol. 18, pp. 929-932, 1977.

[7] R.A. Lobo, J.L. Kelsey and R. Marcus, *Menopause: Biology and Pathobiology*, Academic Press, 2000, pp. 287-307.

[8] A. Rosenberg, *Skeletal system and soft tissue tumors, in Robbins Pathologic Basis of Disease*, 5th edition, R. S. Cotran, V. Kumar and S. L. Robbins (Eds), Philadelphia: W. B. Saunders Co., 1994, pp.1219-1222.

[9] M.F. Holick, "Vitamin D and Bone Health", *J. Nutr*., vol. 126, pp. 1159S-1164S, 1996.

[10] H. Darwish and H.F. DeLuca, "Vitamin D-regulated gene expression", *Crit. Rev. Eukaryotic Gene Express*, Vol. 3, pp. 89-116, 1993.

[11] M.F. Holick, "Vitamin D: new horizons for the 21st century", *Am. J. Clin. Nutr*., vol. 60, pp. 619-630, 1994.

[12] M.F. Holick, "Vitamin D: photobiology, metabolism and clinical applications", in *Endocrinology*, 3rd edition, W.B. Saunders, Philadelphia, PA, 1995, pp. 990-1013.

[13] J.N.M. Heersche and S. Cherk, *Metabolic Bone Disease: cellular and tissue mechanisms*, Boca Raton, FI: CRC Press, 1989.

[14] Y.Y. Kong, H. Yoshida, I. Sarosi, H.L. Tan, E. Timms, C. Capparelli , S. Morony, A. Santos, G. Van, A. Itie, W. Khoo, A. Wakeham, C. Dunstan, D. Lacey, T. Mak, W. Boyle and J. Penninger, "OPGL is a key regulator of osteoclastogenesis, lymphocyte development and lymph-node organogenesis", *Nature*, 397, pp. 315-323, 1999.

[15] N. Takahashi, N. Udagawa and T. Suda, "A new member of tumor necrosis factor ligand family, ODF/ OPGL/ TRANCE/ RANKL, regulates osteoclast differentiation and function", *Biochem. Biophys. Res. Commun*., 256, pp. 449-455, 1999.

[16] T.L. Burgess, Y. Qian, S. Kaufman, B.D. Ring, G. Van, C. Capparelli, M. Kelly, H. Hsu, W.J. Boyle, C.R. Dunstan, S. Hu and D.L. Lacey, "The ligand for osteoprotegerin (OPGL) directly activates mature osteoclasts", *J. Cell Biol*., 145, pp. 527-538, 1999.

[17] J.A. Albright and M. Sauders, *The Scientific Basis of Orthopaedics*, Norwalk, Conn.: Appleton & Lange, 1990.

[18] H.V. Leeuwen, "Vitamin D and differentiation of mesenchymal stem cells and osteoblasts", *Endoc. Abs*., vol. 22, pp. S14.4, 2010.

[19] T.J. Kaper, "An introduction to geometric methods and dynamical systems theory for singular perturbation problems. Analyzing multiscale phenomena using singular perturbation methods", *Proc. Symposia Appl Math*, vol. 56, 1999.

[20] S. Rinaldi and S. Muratori, "A separation condition for the existence of limit cycle in slow-fast systems", Appl Math Modelling, vol. 15, pp. 312-318, 1991.

[21] W. Sanprasert, U. Chundang and M. Podisuk, "Integration method and Runge-Kutta method", in *Proc. 15th American Conf. on Applied Mathematics*, WSEAS Press, Houston, USA, 2009, pp. 232.

[22] M. Racila and J.M. Crolet, "Sinupros: Mathematical model of human cortical bone", in *Proc. 10th WSEAS Inter. Conf. on Mathematics and Computers in Biology and Chemistry*, WSEAS Press, Prague, Czech Republic, 2009, pp. 53.

[23] N. Razali, R. R. Ahmed, M. Darus and A.S. Rambely, "Fifth-order mean Runge-Kutta methods applied to the Lorenz system", in *Proc. 13th WSEAS Inter. Conf. on Applied Mathematics*, WSEAS Press, Puerto De La Cruz, Tenerife, Spain, 2008, pp. 333.

[24] A. Chirita, R. H. Ene, R.B. Nicolescu and R.I. Carstea, "A numerical simulation of distributed-parameter systems", in *Proc. 9th WSEAS Inter. Conf. on Mathematic*al Methods and Computational Techniques in Electrical Engineering, WSEAS Press, Arcachon, 2007, pp. 70.

[25] V. Tangpricha, P. Koutkia, S.M. Rieke, T.C. Chen, A.A. Perez, and M.F. Holick, "Fortification of orange juice with vitamin D: a novel approach for enhancing vitamin D nutritional health", *Am. J. Clin. Nutr*., vol. 77, pp. 1478-1483, 2003.

[26] M.F. Holick, "Sunlight and vitamin D for bone health and prevention of autoimmune diseases, cancers, and cardiovascular disease", *Am. J. Clin. Nutr.*, vol. 80 (suppl), pp. 1678S-1688S, 2004.